JOC The Journal of Organic Chemistry

Article

pubs.acs.org/joc

Long Chalcogen−Chalcogen Bonds in Electron-Rich Two and Four Center Bonds: Combination of π- and σ-Aromaticity to a Three-Dimensional σ/π-Aromaticity

Rolf Gleiter*[,†] and Gebhard Haberhauer*[,‡]

[†]Organisch-Chemisches Institut, Universität Heidelberg, Im Neuenheimer Feld 270, D-69120 Heidelberg, Germany

[‡]Institut für Organische Chemie, Universität Duisburg-Essen, Universitätsstr. 7, D-45117 Essen, Germany

Supporting Information

ABSTRACT: Quantum chemical calculations were carried out by applying density functional theory to study the two center-three electron (2c-3e) bonds between the sulfur centers of cyclic dithioethers. Calculated were the S−S distance, the stabilization energy, and the energy of the $\sigma \rightarrow \sigma^*$ transition. The extension of the calculations to two (2c-3e) bonds in one molecule shows that a rearrangement to one σ bond and two lone pairs on sulfur is usually more favorable. Exceptions are $[H_2S_2^+]_2$, the dimer of the 1,2-dithia-3,5-diazolyl radical (**27a**), the dimer of the 1,2,4-trithia-3,5-diazolyl radical cation (**26a**$^{2+}$), and its Selena congeners and derivatives. In the case of $[H_2S_2^+]_2$, the (4c-6e) bond between the chalcogen centers is a good description of this dimer. To describe the binding situation in the dimer **26a**$^{2+}$ and **27a**, the concept of a "simple" (4c-6e) bond was extended. Our calculations reveal a strong σ-aromaticity within the plane of the four sulfur centers in addition to a strong π-conjugation within the five-membered rings. The whole phenomenon can best be described as a three-dimensional σ/π-aromaticity within the 14π dimers.

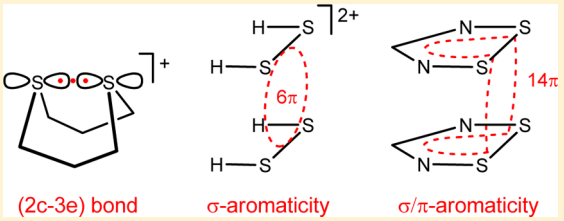

INTRODUCTION

The recent availability of fast correlated ab initio methods made it possible to analyze the quantum mechanical nature of through-space interactions between π electron systems or the interaction between halogen or chalcogen units in molecules. Our calculations on pairs of sulfides, selenides, and tellurides revealed that their mutual chalcogen interactions are mainly due to induction and dispersion forces.[1] These results stimulated again our interest in "long bonds" (>2.2 to 4.0 Å) between divalent chalcogen centers. In this paper, we discuss our recent studies on two center-three electron (2c-3e) bonds and four center-six electron (4c-6e) bonds between chalcogen centers.

RESULTS AND DISCUSSION

Two Center-Three Electron Bonds. In the gas phase, thioethers and dithioethers show ionization energies well below 9 eV.[2] This explains that organic sulfides can be readily oxidized.[3] The one-electron oxidation of the cyclic disulfides **1**−**4** with strong oxidants such as Tl^{2+}, Ag^{2+}, or $NO^+BF_4^-$ yielded the colored radical cations **5**$^{\bullet+}$−**8**$^{\bullet+}$, as summarized in Scheme 1.[3] Such intramolecular complexes were identified by a broad and structureless absorption band with a maximum between 400 and 600 nm. They were interpreted to stem from a $\sigma \rightarrow \sigma^*$ transition.[3] Studies by Asmus[3a] and Musker[3b] revealed that the overlap integral between the 3p orbitals at the sulfur centers correlates with the position of the long wavelength band: the larger the overlap integral, the shorter the wavelength and the higher the energy of the corresponding transition.

Scheme 1. One-Electron Oxidation of the Cyclic Disulfides 1−4 to the Radical Cations 5$^{\bullet+}$**−8**$^{\bullet+}$[a]

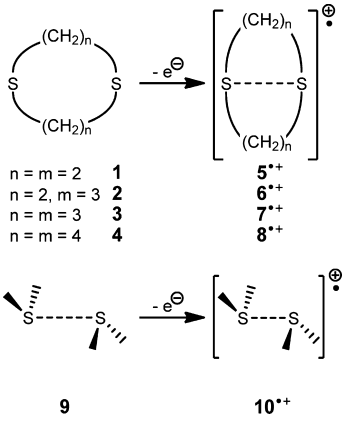

[a]The oxidation of two dimethylsulfides (**9**) to the radical cation **10**$^{\bullet+}$ is shown below.

To derive accurate values for **5**$^{\bullet+}$ to **8**$^{\bullet+}$ and related species, we optimized the geometrical parameters of the molecules by using density functional theory (DFT)[4] applying Becke's[5] three-parameters hybrid functional and the correlation func-

Received: June 7, 2014
Published: July 10, 2014

   dx.doi.org/10.1021/jo501277h | J. Org. Chem. 2014, 79, 7543−7552

tional suggested by Lee, Yang, and Parr (LYP).[6] As basis set, the cc-pVTZ basis[7] was used. UV/vis spectra of the compounds were simulated with time-dependent density functional theory using the B3LYP functional (TD-B3LYP[8]) and the cc-pVTZ basis set.

In connection with the relation to (2c-3e) and (4c-6e) bonds, we were also interested in the strength of the S···S bonds in these model systems. To derive a measure for the S···S bond strength, we calculated the geometrical parameters of the radical cations listed in Figure 1. For each molecule, we list two

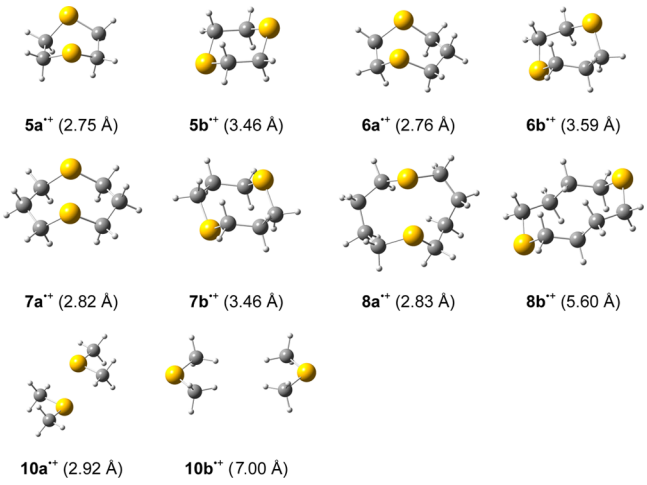

Figure 1. Calculated structures of $\mathbf{5a}^{\bullet+}$/$\mathbf{5b}^{\bullet+}$ to $\mathbf{8a}^{\bullet+}$/$\mathbf{8b}^{\bullet+}$ and $\mathbf{10a}^{\bullet+}$/$\mathbf{10b}^{\bullet+}$. The distances between the sulfur centers are given below the formula.

conformations **a** and **b**. In **a**, a boat-like conformation is adopted which allows the formation of the (2c-3e) bond. In the isomers **b**, the two sulfur centers are as far away from each other as allowed by the skeleton. As a result, $\mathbf{5b}^{\bullet+}$ to $\mathbf{7b}^{\bullet+}$ adopt chair conformations. The difference ΔE between the total energies of **a** and **b** is a measure for the strength of the (2c-3e) bond. These values together with calculated S···S distances and the energy for the long wavelength UV/vis band can be found in Table 1.

Table 1. Calculated S···S Distances for $\mathbf{5}^{\bullet+}$ to $\mathbf{8}^{\bullet+}$ and Energy Differences, ΔE, between Conformations of a and b[a]

			UV/vis		
compound	S···S distance (Å)	ΔE^b (kcal mol^{-1})	(eV)	λ_{calcd} (nm)	λ_{exp} (nm)
$\mathbf{5a}^{\bullet+}$	2.75	0.00	1.91	648	650
$\mathbf{5b}^{\bullet+}$	3.46	0.51			
$\mathbf{6a}^{\bullet+}$	2.76	0.00	2.45	505	470
$\mathbf{6b}^{\bullet+}$	3.59	10.49			
$\mathbf{7a}^{\bullet+}$	2.82	0.00	3.05	406	400
$\mathbf{7b}^{\bullet+}$	3.46	18.60			
$\mathbf{8a}^{\bullet+}$	2.83	0.00	2.76	449	450
$\mathbf{8b}^{\bullet+}$	5.60	19.78			
$\mathbf{10a}^{\bullet+}$	2.92	0.00			
$\mathbf{10b}^{\bullet+}$	7.00[c]	21.30			

[a]The wavelength of the first band in the UV/vis spectra calculated (TD-B3LYP/cc-pVTZ) for $\mathbf{5a}^{\bullet+}$ to $\mathbf{8a}^{\bullet+}$ is compared with the experimental values. [b]B3LYP/cc-pVTZ. [c]The S···S distance was fixed at this value.

The energy difference ΔE increases from $\mathbf{5}^{\bullet+}$ to $\mathbf{6}^{\bullet+}$ and $\mathbf{7}^{\bullet+}$. This can be rationalized by considering the strain energy that arises in $\mathbf{5}^{\bullet+}$ and $\mathbf{6}^{\bullet+}$ through two ($\mathbf{5a}^{\bullet+}$) or one ($\mathbf{6a}^{\bullet+}$) eclipsed C_2H_4 units. In $\mathbf{5a}^{\bullet+}$, the effect of through-bond interactions[9] seems to be rather small because the C−C bond length (1.562 Å) is not far from a "normal" value. In the eight-membered ring of $\mathbf{7a}^{\bullet+}$, the CH_2 groups in the bridges (see Figure 1) adopt a staggered conformation. In $\mathbf{8a}^{\bullet+}$, the two C_4H_8 bridges are almost staggered, which shows up in a ΔE value of 19.8 kcal mol^{-1}. These values suggest a stabilization energy for the (2c-3e) bond between sulfur centers of about 20 kcal mol^{-1}. As anticipated, the values found for the (2c-3e) bond are considerably smaller than the energy for a (2c-2e) S−S bond for which values between 40 and 60 kcal mol^{-1} were calculated.[10] The rather long distance for the (2c-3e) bond in $\mathbf{5a}^{\bullet+}$ to $\mathbf{8a}^{\bullet+}$ can be traced back to a high p character (98% p character according to a NBO analysis[11]) and the fact that the unpaired electron occupies an antibonding (σ^*) orbital. The transannular distances of the chair conformers $\mathbf{5b}^{\bullet+}$ to $\mathbf{7b}^{\bullet+}$ are close to the van der Waals distance for two sulfur centers (3.6−3.8 Å).[12] For the conformer $\mathbf{8b}^{\bullet+}$, the S···S distance is larger due to the longer bridges.

In Table 1, we also list the data for a (2c-3e) bond between $[(CH_3)_2S]_2^{\bullet+}$ ($\mathbf{10}^{\bullet+}$). For our calculations, we adopted a C_{2h} symmetry for $\mathbf{10a}^{\bullet+}$ to avoid severe steric interactions of the methyl groups. For $\mathbf{10b}^{\bullet+}$, D_{2h} symmetry and an S···S distance of 7.0 Å was adopted. The difference between the isomer $\mathbf{10a}^{\bullet+}$ and the conformation $\mathbf{10b}^{\bullet+}$ was calculated to be 21.30 kcal mol^{-1}, which is slightly more than the value for $\mathbf{8a}^{\bullet+}$/$\mathbf{8b}^{\bullet+}$.

In connection with our results on the (2c-3e) bonding between sulfur radical cations, it is interesting to look at the (2c-3e) bonds between nitrogen centers. In Figure 2, we have

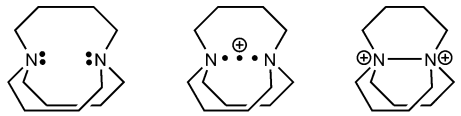

Figure 2. 1,6-Diazabicyclo[4.4.4]tetradecane (**11**) and its mono- ($\mathbf{12}^{\bullet+}$) and dication ($\mathbf{13}^{2+}$). The N···N distances experimentally determined and calculated by means of B3LYP/cc-pVTZ are listed. The latter are in brackets.

listed the N···N distances reported for 1,6-diazabicyclo[4.4.4]-tetradecane (**11**), the monocationic (2c-3e) species $\mathbf{12}^{\bullet+}$, and the dicationic (2c-2e) derivative ($\mathbf{13}^{2+}$).[13] It is interesting to note that the (2c-3e) bond in $\mathbf{12}^{\bullet+}$ is about 50% longer than the (2c-2e) bond in $\mathbf{13}^{2+}$. In the case of $\mathbf{5a}^{\bullet+}$ to $\mathbf{9a}^{\bullet+}$, the lengthening of the S−S bond is about 35% as compared to a S−S single bond (2.02 Å).[14]

The one-electron oxidation of **11** produces the red colored (2c-3e) radical cation $\mathbf{12}^{\bullet+}$, which is rather stable due to the cage formed by the three bridges. The less protected and less strained radical cation $\mathbf{15}^{\bullet+}$ could be generated by pulse radiolysis (Scheme 2).[15] Its decay which is caused by a thermal cleavage of the (2c-3e) bond allowed a measurement of the strength of the central bond in $\mathbf{15}^{\bullet+}$. The measured half-life of 5 ms corresponds to a ΔG value of 14.5 kcal mol^{-1}.[15] This value compares quite well with the calculated ΔG value (see Scheme 2) and the calculated bond strengths of $\mathbf{6a}^{\bullet+}$ to $\mathbf{8a}^{\bullet+}$ as listed in Table 1.

dx.doi.org/10.1021/jo501277h | J. Org. Chem. 2014, 79, 7543−7552

Scheme 2. Generation of $15^{\bullet+}$, a Short-Lived Species with a (2c-3e) Bond[a]

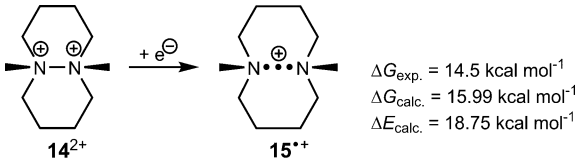

[a]The ΔG and ΔE values for the reaction are listed. The calculated values were obtained using B3LYP/cc-pVTZ.

For the relatively stable cyclic systems $\mathbf{5a}^{\bullet+}$ to $\mathbf{8a}^{\bullet+}$, the electronic spectra have been reported.[3,16] For all of them, the long wavelength band is described as a broad Gaussian shaped band with λ_{max} values in the visible region (see Table 1). The shape of the band suggests that the first excited state is very likely to be antibonding or only weakly bonding with an even longer S−S bond distance than the ground state. The calculated values given in Table 1 compare well with the experiment.

Species with Two (2c-3e) Bonds and (4c-6e) Bonds. In the literature, various disulfides have been proposed as possible candidates for two (2c-3e) bonds in one molecule.[3a] As examples, the species $\mathbf{16}^{2+}$ to $\mathbf{18}^{2+}$ are shown in Scheme 3. In these molecules, the two three-electron bonds are separated from each other. In $\mathbf{19}^{2+}$, as a fourth example, both S···S bonds originate from directly bound S atoms, and we will name them (4c-6e) bonds. The values obtained above for the strength of one (2c-3e) bond (ca. 16−19 kcal mol^{-1}, cf. Table 1) and that of a S−S single bond (40−60 kcal mol^{-1})[10] suggest for the two (2c-3e) bonds of $\mathbf{16}^{2+}$ to $\mathbf{19}^{2+}$ an intramolecular redox reaction resulting in one S−S single bond between two formally positive charged sulfur centers and two nonbonding electron pairs on the divalent sulfur centers as shown for $\mathbf{20}^{2+}$−$\mathbf{25}^{2+}$ in Scheme 3.

Scheme 3. Predicted Rearrangement of $\mathbf{16}^{2+}$−$\mathbf{19}^{2+}$ with Two (2c-3e) Bonds to $\mathbf{20}^{2+}$−$\mathbf{25}^{2+}$, Respectively, with a S−S σ Bond and Two Additional Nonbonding Orbitals on the Neutral Sulfur Centers

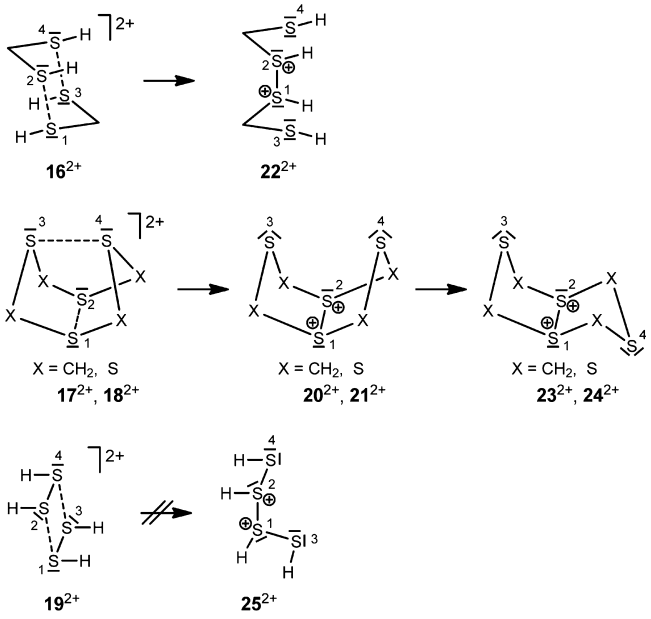

To find out if this assumption is reasonable, we have carried out quantum chemical calculations on $\mathbf{16}^{2+}$ to $\mathbf{19}^{2+}$ and $\mathbf{20}^{2+}$ to $\mathbf{23}^{2+}$ using B3LYP/cc-pVTZ. The results are summarized in Table 2. The open structures $\mathbf{20}^{2+}$ to $\mathbf{24}^{2+}$ are more stable than the corresponding structures with two (2c-3e) bonds, $\mathbf{16}^{2+}$ to $\mathbf{18}^{2+}$. Frequency calculations reveal that the closed structures $\mathbf{17}^{2+}$ and $\mathbf{18}^{2+}$ are transition states and $\mathbf{16}^{2+}$ has two imaginary frequencies. This result is supported by experimental data in the case of $\mathbf{18}^{2+}/\mathbf{24}^{2+}$: the structure of S_8^{2+} has been reported in the literature, and a chair-boat conformation as shown in $\mathbf{24}^{2+}$ was found with a transannular S−S bond of 2.86 Å.[17] With these results, calculations on the nature of transannular interactions in E_4N_4 and E_8^{2+} (E = S, Se) species are in line.[18]

Table 2. Calculated (B3LYP/cc-pVTZ) Structural Properties and Energy Differences between $\mathbf{16}^{2+}$−$\mathbf{19}^{2+}$ and $\mathbf{20}^{2+}$−$\mathbf{25}^{2+}$[a]

compound	S1···S2 distance (Å)	δ(S1)	δ(S3)	ΔE (kcal mol^{-1})
$\mathbf{16}^{2+}$	2.90	0.38	0.38	0.00
$\mathbf{22}^{2+}$	2.56	0.37	0.34	−23.3
$\mathbf{17}^{2+}$	2.92	0.62	0.62	0.00
$\mathbf{20}^{2+}$	2.12	0.65	0.49	−18.7
$\mathbf{23}^{2+}$	2.15	0.69	0.44	−22.1
$\mathbf{18}^{2+}$	3.29	0.24	0.24	0.00
$\mathbf{21}^{2+}$	2.84	0.29	0.18	−4.3
$\mathbf{24}^{2+}$	3.11	0.27	0.17	−11.8
$\mathbf{19}^{2+}$	2.96	0.28	0.28	0.00
$\mathbf{25}^{2+}$	2.68	0.30	0.28	+2.84

[a]The partial charges at S1 and S3 (δ(S1) and δ(S3)) have been derived by NBO analysis.

A completely different situation is found for the conformers $\mathbf{19}^{2+}$ and $\mathbf{25}^{2+}$. Only the C_{2h}-symmetric structure with two (4c-6e) bonds, $\mathbf{19}^{2+}$, represents a stationary point. The open structure $\mathbf{25}^{2+}$, in which the dihedral angle θ(S3−S1−S2−S4) was held at 90° and all other geometric variables were optimized within the C_2 point group, is less stable by +2.84 kcal mol^{-1} (Table 2). To rationalize this unexpected result, we have plotted in Figure 3 the four π-type orbitals of the sulfur centers in $\mathbf{19}^{2+}$ as a function of the S···S distance assuming C_{2h} symmetry.[19] In this MO diagram, the orbitals a_g, b_u, and a_u are occupied with two electrons, and one orbital (b_g) will be empty: a reduction of d, the distance between the two $H_2S_2^+$ units, will stabilize the bonding MOs a_g and a_u and destabilize the antibonding orbitals b_u and b_g. It is interesting to note that the positive slope of a_g and a_u is larger up to d = 3 Å than the negative slope of the antibonding occupied orbital b_u. As a result, the total energy is lowered since nuclear−nuclear repulsion is still small at these distances. The total minimum of the potential energy curve of $\mathbf{19}^{2+}$ is found at 2.96 Å (see also Table 2). A detailed look at the orbital energies shows that the stabilization of the bonding levels a_g and a_u is operative already for relatively long distances, whereas the destabilization of the antibonding b_u orbital is only significant below 3.0 Å. This behavior was traced back to the interaction of the a_u and b_u π orbitals with σ^* orbitals of the same symmetry. As shown in Figure 4, this orbital mixing reduces the antibonding and increases the bonding character of the resulting orbitals.[19]

The unexpected stabilization of $\mathbf{19}^{2+}$ can also be explained by another concept, namely, the σ-conjugation.[20] The four-membered ring, which is formed by the four sulfur centers, has 6π electrons (a_g^2, b_u^2, and a_u^2) and should therefore exhibit σ-aromaticity.[20] In Figure 3, this situation is described by the two valence structures of $\mathbf{19}^{2+}$. Valence structure A represents a "simple" van der Waals bond between the two $H_2S_2^+$ units,

dx.doi.org/10.1021/jo501277h | J. Org. Chem. 2014, 79, 7543−7552

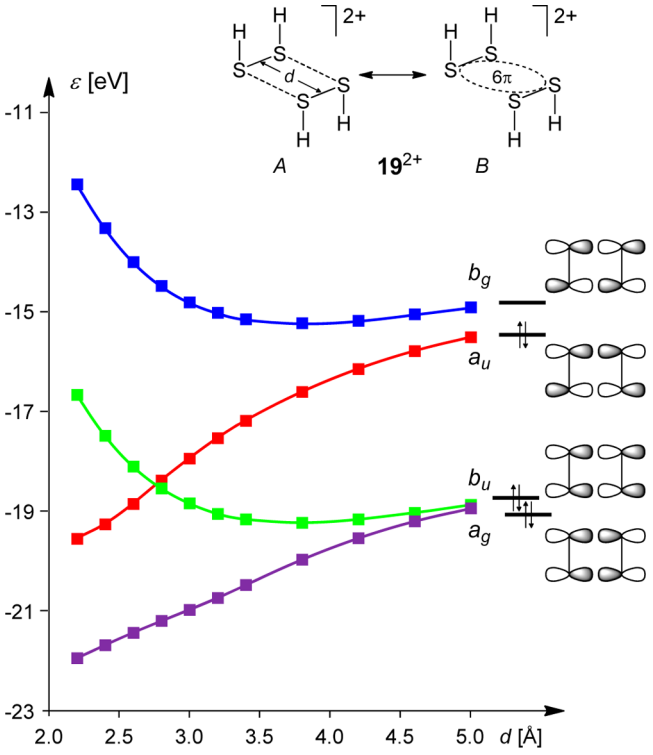

Figure 3. Four p_π orbitals of $[H_2S_2^+]_2$ as a function of distance d, assuming C_{2h} symmetry.

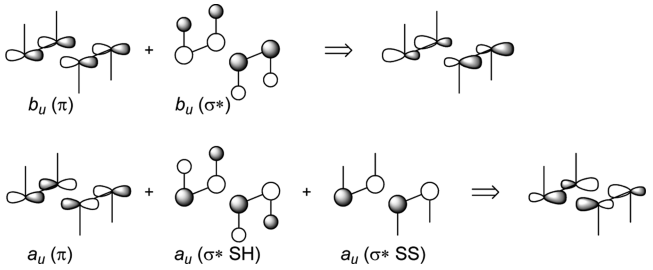

Figure 4. Schematic drawing of the orbital mixing of b_u (π) and a_u (π) with the corresponding σ^* orbital to explain the decreasing antibonding character of b_u and increasing bonding character (a_u) during the reduction of d.

whereas in valence structure B, the (4c-6e) bonds are illustrated as a σ-aromatic unit.[19] An estimation of the σ-aromaticity of $\mathbf{19}^{2+}$ can be made using its NICS values as a measure for the ring current effect.[21] Negative nucleus-independent chemical shifts (NICS) denote aromaticity; positive NICS values denote antiaromaticity. For example, cyclobutane and related molecules with four-membered rings are destabilized by σ-antiaromaticity involving the eight electrons in the strained C−C bonds and therefore exhibit positive NICS values.[22] For cyclobutane (D_{4h}), a NICS(0) value of +3.3 ppm is calculated using B3LYP/cc-pVTZ. The NICS(1) value for cyclobutane amounts to +1.7 ppm. In contrast to this, we found that the calculated (B3LYP/cc-pVTZ) NICS(0) value of $\mathbf{19}^{2+}$ is −19.4 ppm and the NICS(1) value amounts to −10.9 ppm. These results indicate a strong σ-conjugation between the sulfur centers and justify the use of valence structure B for $\mathbf{19}^{2+}$ (see Figure 3).

The compound $\mathbf{19}^{2+}$ has never been experimentally observed, but in the dimers of the 1,2,4-trithia-3,5-diazolyl radical cation ($\mathbf{26a}^{2+}$), the 1,2-dithia-3,5-diazolyl radical (**27a**) as well as in their Selena congeners $\mathbf{26b}^{2+}$ and **27b**, respectively (see Figure 5), which are all stable species in the solid state,[23−25] a structural element is found which resembles the σ-aromatic unit $[H_2S_2^+]_2$. However, the bonding situation in these dimers is even more complicated since the monomers themselves are already π-aromatic rings. In order to understand the bonding within the dimers $\mathbf{26a}^{2+}$ and **27a**, we will start by looking at the electronic structures of their monomers, the 1,2,4-trithia-3,5-diazolyl radical cation ($\mathbf{28}^{\bullet+}$) and the 1,2-dithia-3,5-diazolyl radical ($\mathbf{29}^{\bullet}$). In a first step, we can count the valence electrons of the planar five-membered rings of $\mathbf{28}^{\bullet+}$ and $\mathbf{29}^{\bullet}$. In the case of the radical cation, we encounter four S−N σ bonds and one S−S σ bond, each contributing two electrons. Each center further contributes two nonbonding electrons which are drawn in orbital lobes at the outside of the five-membered ring in Figure 6a. These σ electrons add up to 20, as seen in Figure 6a, which leaves seven π electrons for $\mathbf{28}^{\bullet+}$. The latter are subdivided into two $3p_\pi$ electrons at each sulfur center of the S−S bond, one $3p_\pi$ electron at the third sulfur atom, and one $2p_\pi$ electron at each nitrogen center. These seven π electrons are drawn inside the ring of $\mathbf{28}^{\bullet+}$ as dots in Figure 6a.

In analogy, the electron count for radical $\mathbf{29}^{\bullet}$ leads to six σ bonds (1 S−S, 2 S−N, 2 C−N, 1 C−H), contributing two electrons each and four nonbonding electron pairs. This also adds up to 20 σ electrons and leaves seven π electrons for the neutral radical $\mathbf{29}^{\bullet}$, as shown in Figure 6a.

In Figure 6b, we present a qualitative diagram showing the HMO energies and wave functions of the π systems of $\mathbf{28}^{\bullet+}$ and $\mathbf{29}^{\bullet}$, assuming C_{2v} symmetry for both species. The levels $1a_2$/

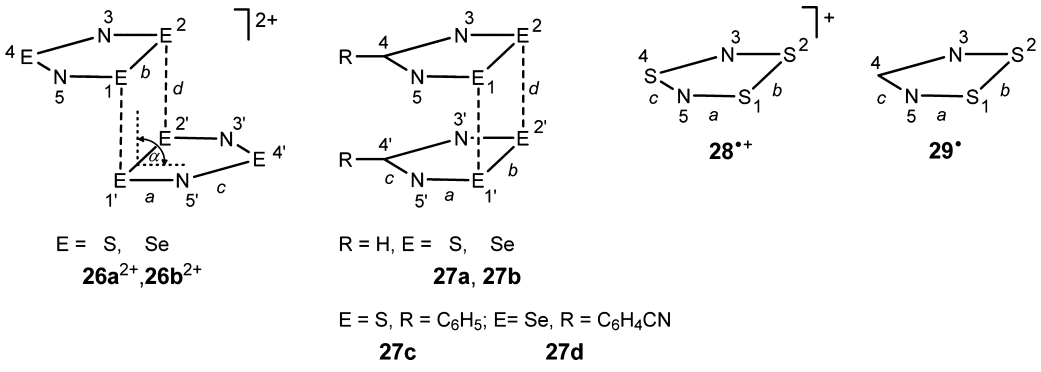

Figure 5. Formulas of dimers $\mathbf{26}^{2+}$ and **27** and the monomers $\mathbf{28}^{\bullet+}$ and $\mathbf{29}^{\bullet}$ for use in connection with the recorded bond length given in Tables 3 and 4.

dx.doi.org/10.1021/jo501277h | J. Org. Chem. 2014, 79, 7543−7552

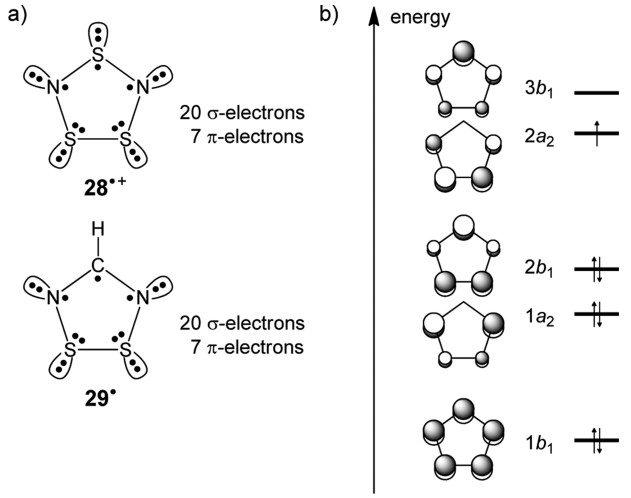

Figure 6. (a) Formal subdivision of the valence electrons of $[S_3N_2]^{\bullet+}$ (**28**$^{\bullet+}$) and $S_2N_2CH^{\bullet}$ (**29**$^{\bullet}$) into σ and π electrons. (b) Qualitative HMO scheme of **28**$^{\bullet+}$ and **29**$^{\bullet}$. For the five-membered rings, C_{2v} symmetry is assumed.

$2b_1$ and $2a_2/3b_1$ are close in energy. This implies that either an $^2A_2$ or a $^2B_1$ state is possible for **28**$^{\bullet+}$ and **29**$^{\bullet}$. Although ESR spectra of **28**$^{\bullet+}$ and **29**$^{\bullet}$, as well as of the 4-methyl- and 4-phenyl-1,2-dithia-3,5-diazolyl radicals **30**$^{\bullet}$ and **31**$^{\bullet}$,[23c,f,24] are available, they are not helpful to discriminate between both states. Because the coefficients of the π-MOs at the nitrogen centers of $2a_2$ and $3b_1$ are very similar (see Figure 6b), we expect similar ^{14}N coupling constants from the ESR experiments.[26] By using polarized neutron diffraction, it was possible to study the spin distribution of a derivative of **29**$^{\bullet}$, the 4-(4-nitro-2,3,5,6-tetrafluorophenyl)-1,2-dithia-3,5-diazolyl radical.[27] The spin density maps obtained show that almost all the spin density is localized on the sulfur and nitrogen atoms and only a small negative spin density is observed on the carbon atom of the 1,2-dithia-3,5-diazolyl ring. These results are in good agreement with ab initio calculations.[27] DFT (B3LYP/cc-pVTZ) calculations also predict the orbital sequence $2a_2$ below $3b_1$ for **28**$^{\bullet+}$ and **29**$^{\bullet}$.

By joining two radicals each of **28**$^{\bullet+}$ or **29**$^{\bullet}$, in such a way that either **26a**$^{2+}$ (C_{2h}) or **27a** (C_{2v}) are generated, 10 π-type orbitals are obtained with bonds between the S−S units. The resulting π orbitals give rise to pairs at large distances d between the two units (Figure 7). These orbital pairs either belong to the irreducible representations a_g/b_u and a_u/b_g in the case of the point group C_{2h} or a_1/b_1 and a_2/b_2 in the point group C_{2v}. In order to perceive the essence of the (4c-6e) bonding in **26a**$^{2+}$ and **27a**, we are presenting in Figure 7 a schematic drawing of the corresponding wave functions of the three highest occupied and lowest unoccupied π-MOs of *anti*-**27a**. For the sake of clarity, we chose the *anti* configuration of the two five-membered rings. We note that the four wave functions are similar at the sulfur part to those encountered in Figure 3 for $[H_2S_2^+]_2$. Two orbitals (a_g, a_u) are bonding and two are antibonding (b_u, b_g) with respect to a S−S interaction between the rings. In Figure 7, we have plotted the energy levels for these four MOs as a function of the distance d between the centers of the S−S bonds of both rings. As in the $[H_2S_2^+]_2$ case, two of the occupied MOs (a_g, a_u) are stabilized when d is reduced, and the third occupied MO (b_u) is destabilized as well as the LUMO (b_g). As a result of this behavior, an energy minimum at a relatively large distance (d = 3 Å) is found for *anti*-**27a**.

In analogy to **19**$^{2+}$ (see Figure 3), *anti*-**27a** can be described by the three valence structures A, B, and C (see Figure 7). Valence structure A represents two five-membered rings each with 7π electrons held together by van der Waals interactions. This valence structure is dominated by the π-aromaticity of the two five-membered rings. In valence structure B, the two five-membered rings are no longer considered as self-contained aromatic units. They split up into two parts: a negatively

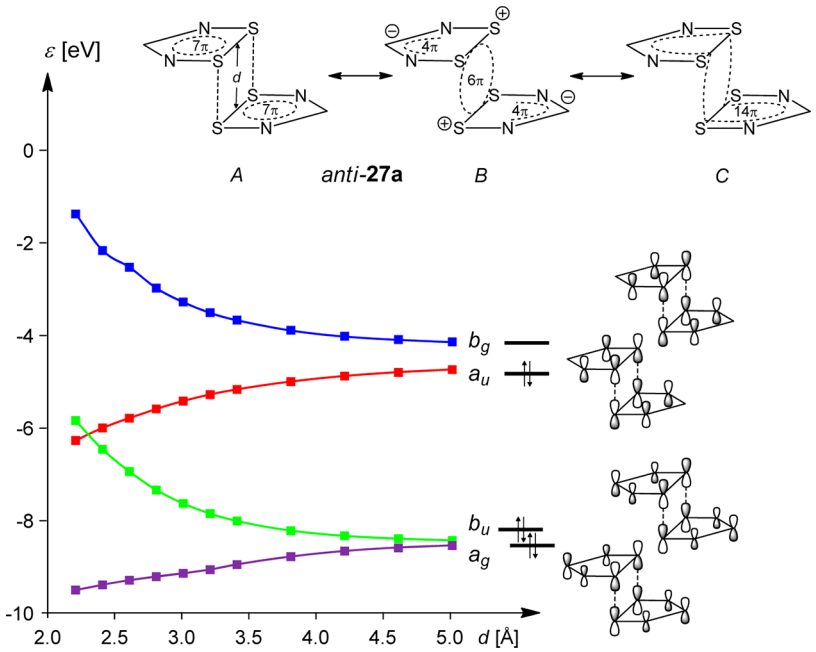

Figure 7. Schematic drawing and energy plot of the lowest unoccupied (b_g) and the highest three occupied π-MOs of *anti*-**27a** as a function of distance d. Energies were calculated using B3LYP/cc-pVTZ.

dx.doi.org/10.1021/jo501277h | J. Org. Chem. 2014, 79, 7543−7552

charged $(N-CH-N)^-$ unit with 4π electrons and a positively charged $(S-S)^+$ unit with 3π electrons. Together with the $(S-S)^+$ unit of the second ring, the latter forms a σ-aromatic system which resembles the σ-aromatic unit in $[H_2S_2^+]_2$. Thus, in valence structure B, the σ-aromaticity is the dominant effect. In valence structure C, the σ- and π-aromaticities of the three rings are combined, forming a three-dimensional σ/π-aromaticity with a total of 14π electrons. In the following, we will discuss the bonding situation in the dimers $\mathbf{26}^{2+}$ and **27** on the basis of experimental data and ab initio calculations, and we will try to clarify which valence structures (A, B, or C) contribute most to the bonding situation in the dimers $\mathbf{26}^{2+}$ and **27**.

In the solid state, the 1,2,4-trithia-3,5-diazolyl radical cation and the 1,2-dithia-3,5-diazolyl radical exist as dimers with long chalcogen−chalcogen bonds, as shown in Figure 5. The dimers of the radical cation ($\mathbf{26}^{2+}$) mostly adopt an *anti* configuration, whereas the neutral dimer **27** prefers the *syn* configuration. The dimers $\mathbf{26a}^{2+}$ and $\mathbf{26b}^{2+}$ have been prepared and investigated by different groups.[23] The bonding between the chalcogen centers of the five-membered rings was interpreted as a (4c-6e) bond,[19,28] which can also be described as 6π σ-aromatic system. This σ-aromaticity of the S_4^{2+} unit in $\mathbf{26a}^{2+}$ was proven by a calculation of the NICS values.[29]

There is extensive literature on **27** and its various substitution products at the carbon center.[25] These molecules came into the focus of chemists in the 1980s and 1990s as possible building blocks for new conducting materials. It was argued that the monomer of a neutral π-radical might give rise to a half-filled energy band in the solid state if the radicals are stacked equally on top of each other.[30] Furthermore, the search for new materials was supported by the possibility to vary the substituent at the carbon center (phenyl, alkyl) in such a way that two- and three-dimensional interactions between the dichalcogenadiazyl units were possible. However, in most cases, the radicals preferred to associate as cofacial dimers (**27a** and **27b**) as drawn in Figure 5.

In Table 3, we have compiled the most relevant structural parameters of $\mathbf{26a}^{2+}$ and $\mathbf{26b}^{2+}$ as well as the 4-phenyl-1,2-dithia-3,5-diazolyl dimer (**27c**)[31] and the 4-(*p*-cyanophenyl)-1,2-diselena-3,5-diazolyl dimer (**27d**).[32] Both structures are shown in Figure 5.

Table 3. Structural Parameters of $\mathbf{26a}^{2+}$, $\mathbf{26b}^{2+}$, 27a, and 27d[a]

	distance (Å)				angle (deg)
compound	*a*	*b*	*c*	*d*	*α*
$\mathbf{26a}^{2+}$	1.61	2.15	1.57	3.00	110.5
$\mathbf{26b}^{2+}$	1.76	2.40	1.70	3.12	106.7
27c	1.63	2.07	1.32	3.11	
27d	1.81	2.32	1.33	3.30	

[a]The distances *a* to *d* (Å) and the angles *α* (deg) between the molecular planes of $\mathbf{26a}^{2+}$ are defined in Figure 5.

The energetic parameters for the dimerization of the radical monomers $\mathbf{28}^{\bullet+}$ to $\mathbf{26a}^{2+}$ could be obtained by measuring the radical concentration as a function of temperature.[24] The ΔH value was reported to be −11.23 kcal mol^{-1}. The energetic parameters for the dimerization of the 4-phenyl-1,2-dithia-3,5-diazolyl radical to **27c** were obtained by the same method.[24] The data obtained for **27c** were $\Delta H = -8.4 \pm 0.1$ kcal mol^{-1} and $\Delta G_{200} = -2.9 \pm 0.2$ kcal mol^{-1}.[24]

The so far published calculations on the structure and binding situation of $\mathbf{26}^{2+}$ and **27** are mainly based on single reference methods.[19,27b,28,29] Here we used for the first time a multireference method, which also includes the dynamic correlation and thus allows the determination of the biradical character and the dimerization energy for the neutral dimer **27a**. As multireference method, we chose the CASPT2[33] approximation, as the underlying CASSCF[34] wave function is able to properly describe biradicals. The dimer **27a** was completely optimized within the C_{2v} point group by means of (8,8)CASPT2/6-311++G**. As the structure without a binding interaction between the two five-membered rings, we used a dimer of $\mathbf{29}^{\bullet}$ ($2 \times \mathbf{29}^{\bullet}$) in which the distance between the aromatic units was held at a value of 7 Å and all other geometric variables were optimized using (8,8)CASPT2/6-311++G** within the C_{2v} point group. Using this method, the dimerization energy was calculated to be −7.38 kcal mol^{-1}, which agrees well with the experimentally observed value for **27c** ($\Delta H = -8.4 \pm 0.1$ kcal mol^{-1}).[24]

An analysis of the CASSCF wave function of the CASPT2 approximation should allow the determination of the biradical character of **27c**. As a measure of the biradical character, the occupation numbers of the frontier orbitals b_1 (HOMO) and a_2 (LUMO) can be used. We found values of 1.50 electrons for b_1 and 0.51 electrons for a_2. In a perfect biradical, both frontier orbitals would be equally populated. For example, we find for the dimer $2 \times \mathbf{29}^{\bullet}$, in which the distance between the aromatic units was held at 7 Å, values of 1.04 electrons for frontier orbital b_1 and 0.96 electrons for frontier orbital a_2. Thus, **27c** is far from being "perfect", and a description of the dimers $\mathbf{26}^{2+}$ and **27** using a single reference method such as DFT is justified. Therefore, we calculated *syn*-$\mathbf{26a}^{2+}$, $\mathbf{26a}^{2+}$, **27a**, *anti*-**27a**, $\mathbf{28}^{\bullet+}$, and $\mathbf{29}^{\bullet}$ using B3LYP as functional and cc-pVTZ as basis set. The calculated distances, the partial charges (δ), and the NICS values are listed in Table 4. The computed values (B3LYP/cc-pVTZ) for the bond lengths within the five-membered rings in $\mathbf{26a}^{2+}$ and **27a** agree very well with the experimental values (see Tables 3 and 4). The distances for the S−S bonds between the ring units in $\mathbf{26a}^{2+}$ and **27a** are also close to the experimental values.

To categorize the measured bond lengths of $\mathbf{26}^{2+}$ and **27** (cf. Table 3), we have listed a selection of molecules as typical examples for formal SN double bonds (**32**, **33**, and **34**), formal SN single bonds (**33** and **35**), and CN aromatic "double bonds" (**36**) in Figure 8. The bond length *c* for $\mathbf{26a}^{2+}$ (1.57 Å) is close to that reported for the SN bond distance in a molecule with SN groups in a conjugated system such as **32** (1.56 Å).[35] Examples of systems with NSN units not conjugating with other π units are **33** (c = 1.54 Å)[36] and **34** (c = 1.50 Å).[37] Both reveal bond orders of about 2 for the NSN group. This comparison between **32**, **33**, and **34** suggests that there is considerable conjugation in the five-membered ring of $\mathbf{26a}^{2+}$. This interpretation is further substantiated when the bond length *a* in $\mathbf{26a}^{2+}$ (1.61 Å) is compared with the formal SN single bonds in **33** (a = 1.70 Å)[36] and **35** (a = 1.66 Å).[38]

For **27c**, we use for a comparison of distance *a* the X-ray data of the cage system **33** and of **35**. The CN bond length *c* of **27c** was compared with *s*-triazine (**36**). The comparison between the formal S−N single bond in **27c** (1.63 Å) with the SN bonds in **33** (a = 1.70 Å)[36] and **35** (a = 1.66 Å)[38] indicates bond shortening by conjugation. This result is supported when bond *c* of **27c** (1.32 Å) was compared with the CN bond of *s*-triazine (1.32 Å).[39] This value corresponds to a bond order of 1.5. This comparison of bond lengths within the five-membered rings of $\mathbf{26a}^{2+}$ and **27c** with model systems **32**−**36** clearly reveals a

dx.doi.org/10.1021/jo501277h | J. Org. Chem. 2014, 79, 7543−7552

Table 4. Calculated Values (B3LYP/cc-pVTZ) for *syn*-**26a**$^{2+}$, **26a**$^{2+}$, **27a**, *anti*-**27a**, **28**$^{\bullet+}$, and **29**$^{\bullet}$[a]

	28$^{\bullet+}$	*syn*-**26a**$^{2+}$	**26a**$^{2+}$	**29**$^{\bullet}$	**27a**	*anti*-**27a**
a (Å)	1.608	1.601	1.601	1.648	1.643	1.642
b (Å)	2.250	2.271	2.272	2.146	2.137	2.140
c (Å)	1.587	1.589	1.589	1.326	1.325	1.326
d (Å)		3.199	3.157		3.126	3.114
δ(S1)/δ(S2)	+0.671	+0.654	+0.652	+0.413	+0.441	+0.452
δ(N3)/δ(N4)	−0.804	−0.805	−0.806	−0.620	−0.652	−0.661
δ(C4) or δ(S4)	+1.267	+1.301	+1.307	+0.211	+0.219	+0.216
NICS(0) (5MR)	−12.41	−19.93	−24.67	−14.53	−18.85	−19.92
NICS(+1) (5MR)	−5.37	−9.45	−13.85	−7.81	−8.58	−10.67
NICS(−1) (5MR)		−12.28	−15.73		−14.31	−12.88
NICS(0) (4MR)		−12.28	−14.70		−13.35	−14.85
NICS(+1) (4MR)		−6.77	−10.55		−8.64	−10.44
NICS(−1) (4MR)		−9.60	−10.55		−12.74	−10.44

[a]The distances are given in Å. The partial charges (δ) are derived by NBO analysis. The NICS (5MR) values are computed for the five-membered rings; the NICS (4MR) values are calculated for the plane defined by the four sulfur atoms. The NICS(+1) values are the NICS(1) values computed 1 Å above the ring and outside the dimer, whereas the NICS(−1) values are the NICS(1) values computed 1 Å above the ring and inside the dimer.

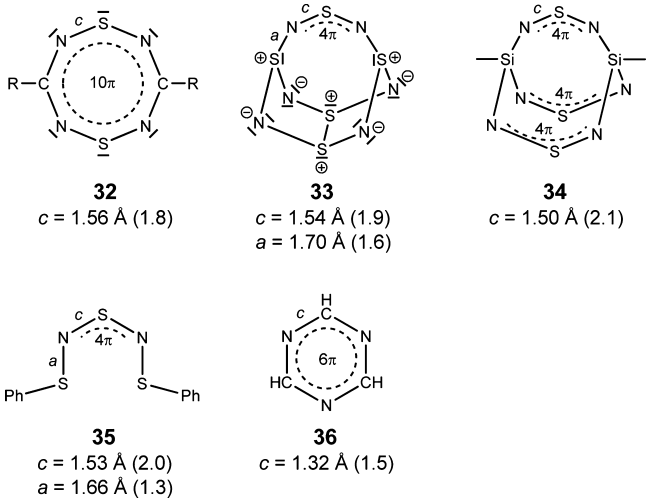

Figure 8. Compounds **32**−**35** with NSN units. The distances *a* and *c* are given with the corresponding bond order in brackets.

considerable π delocalization over the whole ring. These results are a strong argument against valence structure B (see Figure 7) in which a 6π σ-aromatic unit is connected by S−N single bonds to two $(N{-}CH{-}N)^{-}$ units. In this case, we would expect larger values for the distance *a*. A look at the calculated values of *a* shows that no enlargement occurs in the course of the dimerization (**28**$^{\bullet+}$ → *syn*-**26a**$^{2+}$, **28**$^{\bullet+}$ → **26a**$^{2+}$, **29**$^{\bullet}$ → **27a**, and **29**$^{\bullet}$ → *anti*-**27a**) (see Table 4). Furthermore, the NICS values for the five-membered rings [NICS (5MR)] of **28**$^{\bullet+}$, **29**$^{\bullet}$, **26a**$^{2+}$,[29] and **27c** show that the aromaticity of these rings increases, caused by the dimerization, which is in contrast to valence structure B showing no aromatic five-membered rings.

Arguments against valence structure A are the negative NICS values of the four-membered rings [NICS (4MR)] formed by the four sulfur atoms. This we ascribe to a strong σ-conjugation between the $3p_{\sigma}$ orbitals of the four center bond (σ-aromaticity[20]). A hint that the three aromatic units in **27a** are combined to a unique 14π aromatic unit—which corresponds to valence structure C—is the size of the NICS(−1.55) value, which corresponds to the NICS value in the center of complex **27a** and which amounts to −11.55 ppm (Figure 9a). This absolute value is much higher than the NICS(1.55) values of the singular aromatic unit **29**$^{\bullet}$, and it cannot be explained by a simple enhancement caused by three isolated units: Let us

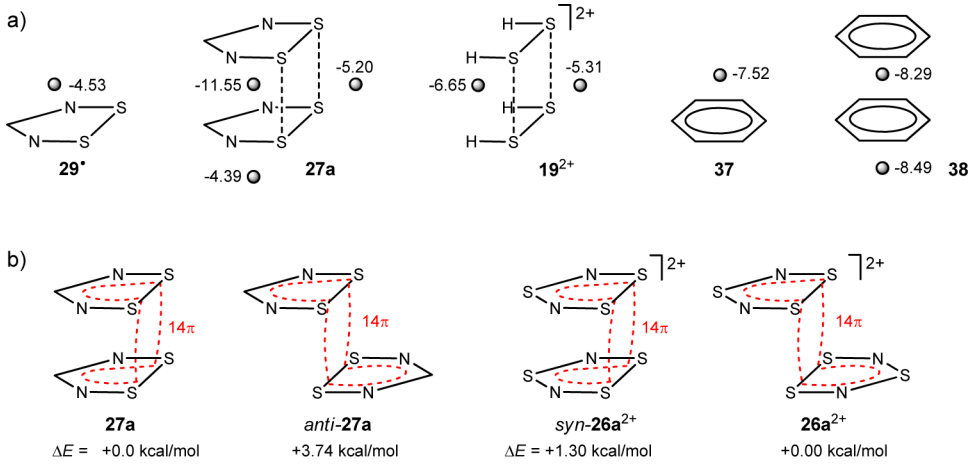

Figure 9. (a) NICS(1.55) values (in ppm) of **19**$^{2+}$, **27a**, **29**$^{\bullet}$, **37**, and **38** calculated using GIAO-B3LYP/cc-pVTZ. (b) Dominant valence structures C in *syn*-**26a**$^{2+}$, **26a**$^{2+}$, **27a**, and *anti*-**27a** representing three-dimensional σ/π-aromatic systems. The relative energies were calculated by means of CCSD(T)/cc-pVTZ//B3LYP/cc-pVTZ.

dx.doi.org/10.1021/jo501277h | J. Org. Chem. 2014, 79, 7543−7552

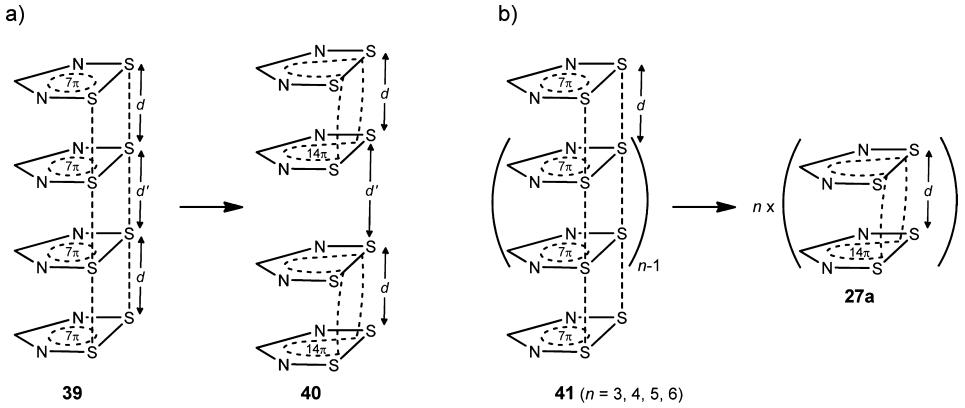

Figure 10. (a) Tetramer **39** consists of four units of **29**$^{\bullet}$ being equidistant. Tetramer **40** consists of two dimers of **27a** showing a distance d' which is larger than the distance d within the dimers **27a**. (b) According to B3LYP/cc-pVDZ calculations, oligomers **41** are unstable compared to separated dimeric units.

consider benzene (**37**) and complex **38** consisting of two benzene units fixed at 3.1 Å (Figure 9a). The NICS(1.55) absolute values of complex **38** consisting of two isolated π systems are only slightly higher than that for benzene. Thus, all data are best in agreement with valence structure C in **27a** representing a three-dimensional σ/π-aromatic system including 10 centers and 14π electrons (Figure 9b). Considering the data in Table 4, it is obvious that the above arguments are also valid for the compounds *syn*-**26a**$^{2+}$, **26a**$^{2+}$, and *anti*-**27a**. Thus, in all these dimers, the valence structures C representing three-dimensional σ/π-aromatic systems are dominant (Figure 9b). Furthermore, we calculated the relative energies of the conformers by means of CCSD(T)/cc-pVTZ//B3LYP/cc-pVTZ. These calculations reveal that, in the case of the cation **26**$^{2+}$, the *anti* configuration is more stable, whereas the neutral dimer **27a** prefers the *syn* configuration. This is in agreement with the experimental observation.

Finally, we would like to briefly discuss the potential use of neutral aromatic radicals such as **29**$^{\bullet}$ as possible building blocks for conducting materials. It was argued that the monomer of a neutral π-radical might give rise to a half-filled energy band in the solid state if the radicals were stacked equally on top of each other.[30] Let us consider a tetramer of **29**$^{\bullet}$: In order to be used as conducting material, this tetramer should consist of four units of **29**$^{\bullet}$ being stacked in an equidistant way (**39** in Figure 10a). However, according to our calculations, two units of **29**$^{\bullet}$ will join to form a σ/π-aromatic dimer **27a**. In this case, we expect the tetramer **40**, which consists of two dimers of **27a** showing a distance d' which is larger than the distance d within the dimers **27a**. To clarify this, we optimized all geometric parameters of a tetramer of **29**$^{\bullet}$ within C_1 symmetry on the level of B3LYP/cc-pVTZ. The calculations show that only the tetrameric system **40** with a very large distance d' (d' > 9 Å and d = 3.13 Å) represents an energetic minimum. To extend this investigation to higher oligomers, we focused our interest on the compounds **41** having 6 to 12 monomeric units of **29**$^{\bullet}$ (Figure 10b). We started the computations with stacks of five-membered rings with equidistant space (d = 3.2 Å) between the rings. The resulting structures were subsequently optimized within C_s symmetry using B3LYP/cc-pVDZ. In all cases, the oligomers **41** were split up into dimers (**27a**) which are separated by more than 8 Å. This allows the conclusion that σ/π-aromaticity dominates and undermines the use of neutral aromatic radicals like **29**$^{\bullet}$ as possible building blocks for conducting materials.

CONCLUSION

Our investigations by means of quantum chemical calculations on (2c-3e) bonds between two divalent sulfur centers reveal a bond energy of about 20 kcal mol^{-1} for the S···S bond in unstrained systems. The calculations reproduce also the energy of the long wavelength band in the electronic absorption spectra very well. The small bond energy of a S···S bond as compared to a S−S single bond (40−60 kcal mol^{-1}) is found to be the reason that the six electrons of two separated (2c-3e) bonds in one molecule convert to one single bond between two positively charged sulfur atoms and two nonbonding electron pairs on divalent sulfur centers via an intramolecular redox reaction. However, two S···S bonds between the sulfur centers of two $H_2S_2^+$ units (**19**$^{2+}$) form stable (4c-6e) bonds. These bonds can also be rationalized by σ-aromaticity which is corroborated by a NICS(1) value of −10.9 ppm. In *anti*-**27a**, where two dithiazolyl radicals are joined together via two adjacent long S···S bonds, our investigations suggest that the resulting tricyclic conjugated molecule can best be described by a three-dimensional aromatic system containing 14π electrons. We also could show that a dimerization of two dithiazolyl radicals is more favorable than a tetramerization with equal distances between the ring units.

COMPUTATIONAL DETAILS

All calculations were performed by using the program packages Gaussian 09[40] and MOLPRO.[41] The geometrical parameters of the radical cations **5a**$^{\bullet+}$−**8a**$^{\bullet+}$, **5b**$^{\bullet+}$−**8b**$^{\bullet+}$, **10a**$^{\bullet+}$, and **10b**$^{\bullet+}$ were optimized by means of density functional theory. For the DFT method, we used the B3LYP[5,6] functional and the cc-pVTZ[7] basis set. For **5a**$^{\bullet+}$−**8a**$^{\bullet+}$ and **5b**$^{\bullet+}$−**7b**$^{\bullet+}$, no symmetry restriction was applied, and for **10b**$^{\bullet+}$ and **10a**$^{\bullet+}$ D_{2h} symmetry and C_{2h} symmetry were applied, respectively. Frequency calculations were carried out at each of the structures (except for **10b**$^{\bullet+}$) to verify the nature of the stationary point. It turned out that all of them are minima. For **10b**$^{\bullet+}$, a S···S distance of 7.0 Å was adopted and all other parameters were optimized within D_{2h} symmetry.

The nitrogen-containing compounds **11**, **12**$^{\bullet+}$, **13**$^{2+}$, and **15**$^{\bullet+}$ were optimized using B3LYP/cc-pVTZ. For the bicycles **11**, **12**$^{\bullet+}$, and **13**$^{2+}$, we assumed D_3 symmetry. For **15**$^{\bullet+}$, we calculated two conformers: For the boat-like conformer, which shows a (2c-3e) bond, C_2 symmetry was applied. The conformer with a maximal distance between the nitrogen centers was calculated using C_i symmetry. Frequency calculations revealed that all structures have no imaginary frequency.

dx.doi.org/10.1021/jo501277h | J. Org. Chem. 2014, 79, 7543−7552

The geometrical parameters of the dicationic species 16^{2+} to 25^{2+} were optimized by means of B3LYP/cc-pVTZ. For 17^{2+}–24^{2+}, no symmetry restriction was applied, and for 16^{2+} and 19^{2+} and for 22^{2+}, C_{2h} symmetry and C_2 symmetry were applied, respectively. Frequency calculations revealed that the closed structures 17^{2+} and 18^{2+} were transition states and 16^{2+} had two imaginary frequencies, whereas 19^{2+} to 24^{2+} have no imaginary frequency. To calculate the open structure 25^{2+}, the dihedral angle θ(S3–S1–S2–S4) was fixed at 90° and all other geometric variables were optimized within the C_2 point group.

The radicals $28^{\bullet+}$ and $29^{\bullet}$ and the corresponding dimers *syn*-$26a^{2+}$, $26a^{2+}$, **27a**, and *anti*-**27a** were optimized using B3LYP/cc-pVTZ. For $28^{\bullet+}$, $29^{\bullet}$, *syn*-$26a^{2+}$, and **27a**, C_{2v} symmetry was applied, and for $26a^{2+}$ and *anti*-**27a**, C_{2h} symmetry was applied. Subsequent frequency calculations showed that all structures are minima. The NICS values[21] for these compounds were calculated using GIAO-B3LYP/cc-pVTZ, and the energies of the dimers *syn*-$26a^{2+}$, $26a^{2+}$, **27a**, and *anti*-**27a** were obtained by means of the CCSD(T)[42] approximation using cc-pVTZ as the basis set. Furthermore, two dimers of $29^{\bullet}$ were optimized by means of (8,8)CASPT2/6-311++G**:[33] The dimer **27a** was completely optimized within the C_{2v} point group. In the reference dimer $2 \times 29^{\bullet}$, the distance between the aromatic units was fixed at value of 7 Å and all other geometric variables were optimized within the C_{2v} point group.

The tetramer **40** was optimized using B3LYP/cc-pVTZ without symmetry restriction. Frequency calculation revealed that the optimized structure of **40** has no imaginary frequency. The oligomers **41** were optimized using B3LYP/cc-pVDZ within C_s symmetry.

The UV spectra of the compounds were simulated with the time-dependent density functional theory (TD-DFT), using the B3LYP functional and the cc-pVTZ basis set. TD-DFT calculations were performed at the optimized ground-state geometry (B3LYP/cc-pVTZ) of the compounds, and the energy, oscillator strength, and rotatory strength were calculated for each of the 100 lowest singlet excitations.

■ ASSOCIATED CONTENT

Supporting Information

Cartesian coordinates and absolute energies for all calculated compounds. This material is available free of charge via the Internet at http://pubs.acs.org.

■ AUTHOR INFORMATION

Corresponding Authors

*E-mail: rolf.gleiter@oci.uni-heidelberg.de.

*E-mail: gebhard.haberhauer@uni-due.de.

Notes

The authors declare no competing financial interest.

■ ACKNOWLEDGMENTS

This work was supported by the Deutsche Forschungsgemeinschaft (DFG). We would like to thank Dr. Birgit Essen (Bonn), Sascha Woitschetzki, and Petra Krämer for helpful support.

■ REFERENCES

(1) (a) Bleiholder, C.; Werz, D. B.; Köppel, H.; Gleiter, R. *J. Am. Chem. Soc.* **2006**, *128*, 2666–2674. (b) Bleiholder, C.; Gleiter, R.; Werz, D. B.; Köppel, H. *Inorg. Chem.* **2007**, *46*, 2249–2260.

(2) Gleiter, R.; Spanget-Larsen, J. *Top. Curr. Chem.* **1979**, *86*, 139–195.

(3) (a) Asmus, K.-D. *Acc. Chem. Res.* **1979**, *12*, 436–442. (b) Musker, W. K. *Acc. Chem. Res.* **1980**, *13*, 200–206.

(4) Kohn, W.; Sham, L. J. *Phys. Rev. A* **1965**, *140*, 1133–1138.

(5) Becke, A. D. *Phys. Rev. A* **1988**, *38*, 3098.

(6) (a) Lee, C.; Yang, W.; Parr, R. G. *Phys. Rev. B* **1988**, *37*, 785. (b) Miehlich, B.; Savin, A.; Stoll, H.; Preuss, H. *Chem. Phys. Lett.* **1989**, *157*, 200–206.

(7) (a) Dunning, T. H., Jr. *J. Chem. Phys.* **1989**, *90*, 1007–1023. (b) Kendall, R. A.; Dunning, T. H., Jr.; Harrison, R. J. *J. Chem. Phys.* **1992**, *96*, 6796–6806. (c) Woon, D. E.; Dunning, T. H., Jr. *J. Chem. Phys.* **1993**, *98*, 1358–1371. (d) Peterson, K. A.; Woon, D. E.; Dunning, T. H., Jr. *J. Chem. Phys.* **1994**, *100*, 7410–7415.

(8) Bauernschmitt, R.; Ahlrichs, R. *Chem. Phys. Lett.* **1996**, *256*, 454–464.

(9) (a) Bock, H.; Wagner, G. *Angew. Chem., Int. Ed. Engl.* **1972**, *11*, 150–151. (b) Sweigart, D. A.; Turner, D. W. *J. Am. Chem. Soc.* **1972**, *94*, 5599–5603. (c) Gleiter, R.; Haberhauer, G. *Aromaticity and Other Conjugation Effects*; Wiley-VCH: Weinheim, Germany, 2012; Chapter 4.

(10) Denk, M. K. *Eur. J. Inorg. Chem.* **2009**, *2009*, 1358–1368.

(11) Reed, A. E.; Curtiss, L. A.; Weinhold, F. *Chem. Rev.* **1988**, *88*, 899–926.

(12) Bondi, A. *J. Phys. Chem.* **1964**, *68*, 441–451.

(13) Alder, R. W.; Orpen, A. G.; White, J. M. *J. Chem. Soc., Chem. Commun.* **1985**, 949–951.

(14) Hordvik, A. *Acta Chem. Scand.* **1966**, *20*, 1885–1891.

(15) Nelsen, S. F.; Alder, R. W.; Sessions, R. B.; Asmus, K.-D.; Hiller, K.-O.; Goebl, M. *J. Am. Chem. Soc.* **1980**, *102*, 1429–1430.

(16) Asmus, K.-D.; Gillis, H. A.; Teather, G. G. *J. Phys. Chem.* **1978**, *82*, 2677–2682.

(17) Davies, C. G.; Gillespie, R. J.; Park, J. J.; Passmore, J. *Inorg. Chem.* **1971**, *10*, 2781–2784.

(18) Moilanen, J.; Karttunen, A. J.; Tuononen, H. M.; Chivers, T. *J. Chem. Theory Comput.* **2012**, *8*, 4249–4258.

(19) Gleiter, R.; Bartetzko, R.; Hofmann, P. *Z. Naturforsch.* **1980**, *35b*, 1166–1170.

(20) (a) Dewar, M. J. S. *J. Am. Chem. Soc.* **1984**, *106*, 669–682. (b) Cremer, D.; Kraka, E. *J. Am. Chem. Soc.* **1985**, *107*, 3800–3810. (c) Exner, K.; Schleyer, P. v. R. *J. Phys. Chem. A* **2001**, *105*, 3407–3416.

(21) (a) Schleyer, P. v. R.; Maerker, C.; Dransfeld, A.; Jiao, H.; van Eikema Hommes, N. J. R. *J. Am. Chem. Soc.* **1996**, *118*, 6317–6318. (b) Chen, Z.; Wannere, C. S.; Corminboeuf, C.; Puchta, R.; Schleyer, P. v. R. *Chem. Rev.* **2005**, *105*, 3842–3888. (c) Gleiter, R.; Haberhauer, G. *Aromaticity and Other Conjugation Effects*; Wiley-VCH: Weinheim, Germany, 2012; Chapter 1.

(22) (a) Moran, D.; Manoharan, M.; Heine, T.; Schleyer, P. v. R. *Org. Lett.* **2003**, *5*, 23–26. (b) Li, Z.-H.; Moran, D.; Fan, K.-N.; Schleyer, P. v. R. *J. Phys. Chem. A* **2005**, *109*, 3711–3716.

(23) (a) Zalkin, A.; Hopkins, T. E.; Templeton, D. H. *Inorg. Chem.* **1966**, *5*, 1767–1770. (b) Banister, A. J.; Clarke, H. G.; Rayment, I.; Shearer, H. M. M. *Inorg. Nucl. Chem. Lett.* **1974**, *10*, 647–654. (c) Gillespie, R. J.; Ireland, P. R.; Vekris, J. E. *Can. J. Chem.* **1975**, *53*, 3147–3152. (d) Steudel, R.; Rose, F.; Reinhardt, R.; Bradaczek, H. *Z. Naturforsch.* **1977**, *32b*, 488–494. (e) Krebs, B.; Henkel, G.; Pohl, S.; Roesky, H. W. *Chem. Ber.* **1980**, *113*, 226–232. (f) Gillespie, R. J.; Kent, J. P.; Sawyer, J. F. *Inorg. Chem.* **1981**, *20*, 3784–3799. (g) Awere, E. G.; Passmore, J.; White, P. S.; Klapötke, T. *J. Chem. Soc., Chem. Commun.* **1989**, 1415–1417.

(24) Fairhurst, S. A.; Johnson, K. M.; Sutcliffe, L. H.; Preston, K. F.; Banister, A. J.; Hauptman, Z. V.; Passmore, J. *J. Chem. Soc., Dalton Trans.* **1986**, 1465–1472.

(25) (a) Banister, A. J.; Rawson, J. M. *The Chemistry of Inorganic Ring Systems*; Steudel, R., Ed.; Elsevier: Amsterdam, 1992; Vol. *14*, Chapter 17. (b) Cordes, A. W.; Haddon, R. C.; Oakley, R. T. *The Chemistry of Inorganic Ring Systems*; Steudel, R., Ed.; Elsevier: Amsterdam, 1992; Vol. *14*, Chapter 16. (c) Rawson, J. M.; Banister, A. J.; Lavender, I. *Adv. Heterocycl. Chem.* **1995**, *62*, 137–247. (d) Chivers, T. *A Guide to Chalcogen–Nitrogen Chemistry*; World Scientific: River Edge, NJ, 2005.

(26) Gerson, F.; Huber, W. *Electron Spin Resonance Spectroscopy of Organic Radicals*; Wiley-VCH: Weinheim, Germany, 2003.

(27) (a) Luzón, J.; Campo, J.; Palacio, F.; McIntyre, G. J.; Goeta, A. E.; Ressouche, E.; Pask, C. M.; Rawson, J. M. *Physica B* **2003**, *335*, 1–5. (b) Rawson, J. M.; Luzon, J.; Palacio, F. *Coord. Chem. Rev.* **2005**, *249*, 2631–2641.

(28) Höfs, H.-U.; Bats, J. W.; Gleiter, R.; Hartmann, G.; Mews, R.; Eckert-Maksić, M.; Oberhammer, H.; Sheldrick, G. M. *Chem. Ber.* **1985**, *118*, 3781–3804.

(29) Zhang, Q.; Yue, S.; Lu, X.; Chen, Z.; Huang, R.; Zheng, L.; Schleyer, P. v. R. *J. Am. Chem. Soc.* **2009**, *131*, 9789−9799.
(30) (a) Haddon, R. C. *Nature* **1975**, *256*, 394−396. (b) Cordes, A. W.; Haddon, R. C.; Oakley, R. T. *Adv. Mater.* **1994**, *6*, 798−802.
(31) Vegas, A.; Pérez-Salazar, A.; Banister, A. J.; Hey, R. G. *J. Chem. Soc., Dalton Trans.* **1980**, 1812−1815.
(32) Cordes, A. W.; Haddon, R. C.; Hicks, R. G.; Oakley, R. T.; Palstra, T. T. M. *Inorg. Chem.* **1992**, *31*, 1802−1808.
(33) Celani, P.; Werner, H.-J. *J. Chem. Phys.* **2000**, *112*, 5546−5557.
(34) (a) Knowles, P. J.; Werner, H.-J. *Chem. Phys. Lett.* **1985**, *115*, 259−267. (b) Werner, H. J.; Knowles, P. J. *J. Chem. Phys.* **1985**, *82*, 5053−5063.
(35) Ernest, I.; Holick, W.; Rihs, G.; Schomburg, D.; Shoham, G.; Wenkert, D.; Woodward, R. B. *J. Am. Chem. Soc.* **1981**, *103*, 1540−1544.
(36) (a) Chivers, T.; Proctor, J. *J. Chem. Soc., Chem. Commun.* **1978**, 642−643. (b) Roesky, H. W.; Rao, M. N. S.; Nakajima, T.; Sheldrick, W. S. *Chem. Ber.* **1979**, *112*, 3531−3537.
(37) Roesky, H. W.; Witt, M.; Krebs, B.; Henkel, G.; Korte, H.-J. *Chem. Ber.* **1981**, *114*, 201−208.
(38) Leitch, J.; Nyburg, S. C.; Armitage, D. A.; Clark, M. J. *J. Cryst. Mol. Struct.* **1973**, *3*, 337−342.
(39) Wheatley, P. J. *Acta Crystallogr.* **1955**, *8*, 224−226.
(40) Frisch, M. J.; Trucks, G. W.; Schlegel, H. B.; Scuseria, G. E.; Robb, M. A.; Cheeseman, J. R.; Scalmani, G.; Barone, V.; Mennucci, B.; Petersson, G. A.; Nakatsuji, H.; Caricato, M.; Li, X.; Hratchian, H. P.; Izmaylov, A. F.; Bloino, J.; Zheng, G.; Sonnenberg, J. L.; Hada, M.; Ehara, M.; Toyota, K.; Fukuda, R.; Hasegawa, J.; Ishida, M.; Nakajima, T.; Honda, Y.; Kitao, O.; Nakai, H.; Vreven, T.; Montgomery, J. A., Jr.; Peralta, J. E.; Ogliaro, F.; Bearpark, M.; Heyd, J. J.; Brothers, E.; Kudin, K. N.; Staroverov, V. N.; Kobayashi, R.; Normand, J.; Raghavachari, K.; Rendell, A.; Burant, J. C.; Iyengar, S. S.; Tomasi, J.; Cossi, M.; Rega, N.; Millam, N. J.; Klene, M.; Knox, J. E.; Cross, J. B.; Bakken, V.; Adamo, C.; Jaramillo, J.; Gomperts, R.; Stratmann, R. E.; Yazyev, O.; Austin, A. J.; Cammi, R.; Pomelli, C.; Ochterski, J. W.; Martin, R. L.; Morokuma, K.; Zakrzewski, V. G.; Voth, G. A.; Salvador, P.; Dannenberg, J. J.; Dapprich, S.; Daniels, A. D.; Farkas, Ö.; Foresman, J. B.; Ortiz, J. V.; Cioslowski, J.; Fox, D. J. *Gaussian 09*, revision A.02; Gaussian Inc.: Wallingford, CT, 2009.
(41) Werner, H.-J.; Knowles, P. J.; Knizia, G.; Manby, F. R.; Schütz, M.; Celani, P.; Korona, T.; Lindh, R.; Mitrushenkov, A.; Rauhut, G.; Shamasundar, K. R.; Adler, T. B.; Amos, R. D.; Bernhardsson, A.; Berning, A.; Cooper, D. L.; Deegan, M. J. O.; Dobbyn, A. J.; Eckert, F.; Goll, E.; Hampel, C.; Hesselmann, A.; Hetzer, G.; Hrenar, T.; Jansen, G.; Köppl, C.; Liu, Y.; Lloyd, A. W.; Mata, R. A.; May, A. J.; McNicholas, S. J.; Meyer, W.; Mura, M. E.; Nicklass, A.; O'Neill, D. P.; Palmieri, P.; Peng, D.; Pflüger, K.; Pitzer, R.; Reiher, M.; Shiozaki, T.; Stoll, H.; Stone, A. J.; Tarroni, R.; Thorsteinsson, T.; Wang, M. *MOLPRO*, version 2012.1, 2012; a package of ab initio programs; see http://www.molpro.net.
(42) Raghavachari, K.; Trucks, G. W.; Pople, J. A.; Head-Gordon, M. *Chem. Phys. Lett.* **1989**, *157*, 479−483.